Structure of the First Solvation Shell of the Hydroxide Anion. A Model Study Using $OH^-(H_2O)_n$ (n = 4, 5, 6, 7, 11, 17) Clusters

Juan J. Novoa,* Fernando Mota, Carlos Perez del Valle,† and Marc Planas

Department Química Física, Facultat Química, University Barcelona, Av. Diagonal 647, 08028-Barcelona, Spain

Received: March 6, 1997; In Final Form: July 28, 1997[⊗]

The optimum structure of the $OH^-(H_2O)_n$ (n = 4, 5) anionic clusters is studied in a systematic way to locate all its minimum energy conformations. The Becke−Lee−Yang−Parr (BLYP) methodology and the 6−31+G-(2d,2p) basis set is used. Two stable conformers of the $OH^-(H_2O)_4$ cluster have been found, one with three waters solvated to the OH^- oxygen and another with four waters solvating the same oxygen. The trisolvated structure is more stable by 1.24 kcal/mol. The transition state connecting these two conformers lies 2.41 kcal/mol above the trisolvated structure and 1.16 kcal/mol above the tetrasolvated one. Therefore, both conformers should coexist at room temperature. For the OH^- $(H_2O)_5$ cluster, our study has found tri-, tetra-, and pentasolvated minimum energy conformers, although the latter one is not likely to be found at room temperature due to its much lower stability and the negligible barrier it presents when it distorts into the tetrasolvated conformer. The energetics for attaching a water molecule to the OH^- hydrogen of the $OH^-(H_2O)_3$ and $OH^-(H_2O)_4$ clusters has also been explored at the BLYP/6-31+G(2d,2p) level. It is shown that a water in that position is energetically stable when its two hydrogens point to the OH^- hydrogen. However, such a conformation is not a minimum energy structure on the potential energy surface, because the water drifts to become attached to one of the first solvation shell waters. The reason is the much higher stability of the second conformer. It is shown that one can avoid this shift by adding enough water molecules to link the water attached to the OH^- hydrogen with those on the first solvation shell of the $OH^-(H_2O)_3$ cluster. This is is successfully accomplished in the $OH^-(H_2O)_{17}$ cluster, whose optimum Hartree−Fock structure presents four waters coordinated to the OH^- oxygen and one more water coordinated to its hydrogen, thus making the total solvation number of the OH^- in this cluster equal to 5. Structures with solvation numbers equal to four are found. However, pentacoordinated OH^- anions are not found in the smaller n = 7 or 11 clusters studied here.

Introduction

The amount of information available on the structure of the hydroxide anion (OH^-) in water solutions is not very large at the present moment. Part of it comes from spectroscopic studies of aqueous alkali metal hydroxides.[1−3] These studies provide information on the structure of the OH^- anion in solution, which indicates that the OH^- group is not strongly bonded through its hydrogen but makes strong intermolecular water contacts through its oxygen. Other source of experimental information has been the study of the properties of the $OH^-(H_2O)_n$ clusters.[4−10] Clusters of up to n = 60 have been investigated.[10] These cluster studies have shown the presence of "magic numbers", that is, values of n for which the $OH^-(H_2O)_n$ cluster is energetically much more stable than the $n + 1$ and $n - 1$ clusters. These studies also suggest the presence of a shell effect after n = 3, a fact that has been used to conclude that 3 is the number of water molecules in the first solvation shell of the OH^- ion, each located in the positions where one of the lone pairs of the oxygen atoms stands in an sp^3 hybridization. However, no direct information on the geometrical structures of the clusters is available.

Although most computations done up to now have focused their attention in the $n \leq 3$ $OH^-(H_2O)_n$ clusters, there are also some studies on larger clusters. Many computations[11−19] have been aimed at finding the most stable structure of the $OH^-(H_2O)_3$ clusters, as it defines the solvation number of the OH^- anion, and reproducing the shell effect after n = 3 in the incremental association enthalpy. These studies indicate that the first solvation shell of the OH^- anion is constituted by three water molecules. Furthermore, the noncorrelated and correlated ab initio methods give similar structures and stabilities for the conformers of the $OH^-(H_2O)_3$ cluster. However, there are some small differences between the computed and experimental binding energies for the noncorrelated results. Xantheas[19] has recently shown that these discrepancies disappear when the correlation is included at the MP2/aug-cc-pVDZ level.[20] For the $n > 3$ clusters, the number of ab initio computations is very small, only limited to the $OH^-(H_2O)_4$ and $OH^-(H_2O)_6$ clusters.[21] For the first cluster, the most interesting conclusion is that an isolated water molecule attached to the OH^- hydrogen is not a minimum energy structure. Instead, the minimum energy structures are for conformers in which the fourth water is attached to the first solvation shell waters of the $OH^-(H_2O)_3$ cluster, thus starting the second solvation shell. This is in good agreement with the fact that three is the solvation number for the OH^- anion. Concerning the $OH^-(H_2O)_6$ cluster, it has a minimum energy structure resulting from adding three waters attached to the first solvation shell of the $OH^-(H_2O)_3$ cluster.

A recent ab initio molecular dynamics (MD) study[22] of a OH^- anion embedded in a 31-water cluster has questioned some of the previous conclusions on the maximum number of waters that can be directly corrdinated to the OH^- anion. The analysis of the trajectories in that study shows conformations in which the OH^- anion is surrounded by four and even five water

† Current address: LPPM, University Paris-Sud, 91405-Orsay Cedex, France.

⊗ Abstract published in *Advance ACS Abstracts,* September 15, 1997.

S1089-5639(97)00857-8 CCC: $14.00

molecules, all directly attached to the OH^- anion, which suggests the presence of conformations in which the coordination number of the OH^- anion is five, four attached to the oxygen end and one more attached to the hydrogen end. There is an apparent contradiction between these structures and the conclusions from the previous nondynamical studies. Is this a consequence of the methodology employed and the better sampling of the potential energy surface? Is it, instead, due to the cluster size? Are the tetra- and pentasolvated clusters stable when smaller water molecules are present? What is the relative stability of these possible tetra- and pentasolvated clusters compared to the tri-solvated ones? The answer to the previous questions is not only important to understand the structure and solvation number of the solvated OH^- ions but also has major implications for the analysis and design of molecular charge-transfer crystals, which is governed by the same intermolecular rules valid in the $OH^-(H_2O)_n$ clusters. In particular, it affects the commonly accepted empirical rule which states that the maximum number of contacts that a molecule can make is equal to the number of free lone pairs it has, a rule that implies that the maximum number of waters which can be solvated to a OH^- anion is equal to three. Therefore, a detailed study addressing the previous questions seems necessary.

As already pointed out, the MD study indicates that some of the waters attach to the OH^- anion through its hydrogen end, in clear contradiction with the finding from previous ab initio computations.[21] This fact is significant to understand the water reorganization process which can take place in the OH^- hydrogen region when the OH^- anion and its X^+ counterpart are formed from the neutral XOH system.[22−25] The existence of solvent rearrangement is due to the different attraction felt by the water molecule attached to the OH^- hydrogen compared to the one it felt when attached to the XOH molecule. Consequently, knowing the energetics of the $H_{(OH^-)}\cdots$water interaction is fundamental to define the feasibility and extension of this rearrangement. This solvent rearrangement process is thought to be essential to understand some properties of the proton transfer in water:

$$H_2O + H_2O \rightleftharpoons OH^- + H_3O^+ \qquad (1)$$

It can also be important to rationalize the mechanism of acid−base reactions, the reverse of reaction 1, a process in which a water molecule is formed from the OH^- and H_3O^+ fragments. Reaction 1 is highly endothermic in the gas phase but as was recently shown,[26−28] lies within the range of thermal accessible energies when a small number of water molecules (just three) are placed between the two contraions to form a trigonal bypiramidal $OH^-(H_2O)_3H_3O^+$ cluster. The neutral reactant in this process is the neutral $H_2O(H_2O)_3H_2O$ cluster. Similar behavior was also found for some $XH(H_2O)_3H_2O$ clusters (XH = HCl, H_2S, or HF)[27,28] and for the $NH_3(H_2O)_3H_2O$ cluster.[28,29] These clusters are too small to describe the solvent reorganization which can take place once the double ionic forms are produced in solution, but are a first step in this direction. So, the lessons learned in the present study are also relevant to define larger $XH(H_2O)_nH_2O$ clusters in which the possible solvent rearrangement effects are taken into account.

Given the importance of the issues raised above, we decided to carry out a detailed systematic study on the structure and stability of tetra- and pentasolvated OH^- clusters, using the BLYP method and various $OH^-(H_2O)_n$ model clusters. We will show that there are two minimum energy conformers for the OH^- $(H_2O)_4$ cluster, one with a tetrasolvated OH^- oxygen and another with a tri-solvated OH^- oxygen plus a second solvation water. The transition state connecting these two forms will be computed and properly characterized. We will then do a similar study for the OH^- $(H_2O)_5$ cluster to test the possibility of having pentasolvated OH^- oxygen conformers. Then, the energetics for the addition of a water molecule to the OH^- hydrogen of the $OH^-(H_2O)_3$ and $OH^-(H_2O)_4$ clusters will be investigated. We will show that an isolated water molecule is not stable attached to the OH^- hydrogen in any of the latter two clusters. However, the water molecule attached to the OH^- hydrogen is a minimum energy structure when its drift toward the first solvation shell is avoided. One way of doing this is by the inclusion of water molecules which connect the water attached to the OH^- hydrogen with those in the first solvation shell, as in the $OH^-(H_2O)_{17}$ cluster, a cluster in which the OH^- anion can be pentacoordinated.

Computational Details

The density functional methodology[30] has shown its potential in tackling problems in which the correlation contribution is not negligible and the size of the system makes impractical the use of the second-order Moller−Plesset or more elaborated correlated methods.[31] Among the various density functionals nowadays available, the Becke−Lee−Yang−Parr functional (abbreviated BLYP) is one of the most promising ones. This functional is a combination of the gradient-corrected Becke[32] exchange functional and the Lee−Yang−Parr[33] correlation functional. A previous study has shown that the BLYP functional gives for the OH^- $(H_2O)_n$ ($n = 1-3$) clusters results similar in quality to the MP2 method.[34] Therefore, we choose such a functional to compute the optimum energy structure and relative stability of the various conformers of the $OH^-(H_2O)_n$ clusters studied here.

We have used the BLYP functional as implemented in the Gaussian-94 suite of programs.[35] The basis set employed is the standard Gaussian contracted 6-31+G(2d,2p) basis set.[36] Except when otherwise noted, the geometry of each cluster is fully optimized imposing no geometrical or symmetry restrictions on its structure. The true minimum nature of the optimum geometry will be confirmed for the most interesting clusters by performing a harmonic vibrational analysis.

Many of the clusters selected here present a rather complex network of hydrogen bond intermolecular interactions. This makes it very difficult to identify these bonds by simple inspection of the structure of the cluster. Therefore, we decided to carry out a topological analysis of the electronic density, to locate the bond critical points present in the cluster.[37] The bond critical points, also called (3,−1) points, are placed in the region between the atoms involved in the intermolecular contact. These points correspond to places where the gradient of the density is zero with respect to all the coordinates and, at the same time, the second derivative matrix of that density has one positive and two negative eigenvalues. The presence or absence of this type of points defines the presence of a hydrogen bond between some atoms.[37] The topological analysis was carried out by using the appropriate options in Gaussian-94[38] or the EXTREME program.[39]

Results and Discussion

Structure and Stability of the $OH^-(H_2O)_4$ Cluster. One way of locating the optimum structure of the $OH^-(H_2O)_4$ cluster is by looking at the most stable conformations of the cluster as a function of the distance between the approaching water and the $OH^-(H_2O)_3$ cluster. The interaction between these two subsystems is essentially one between a negatively charged ion and a permanent dipole; that is, it has a strong electrostatic character. Consequently, it's possible to have a good qualitative

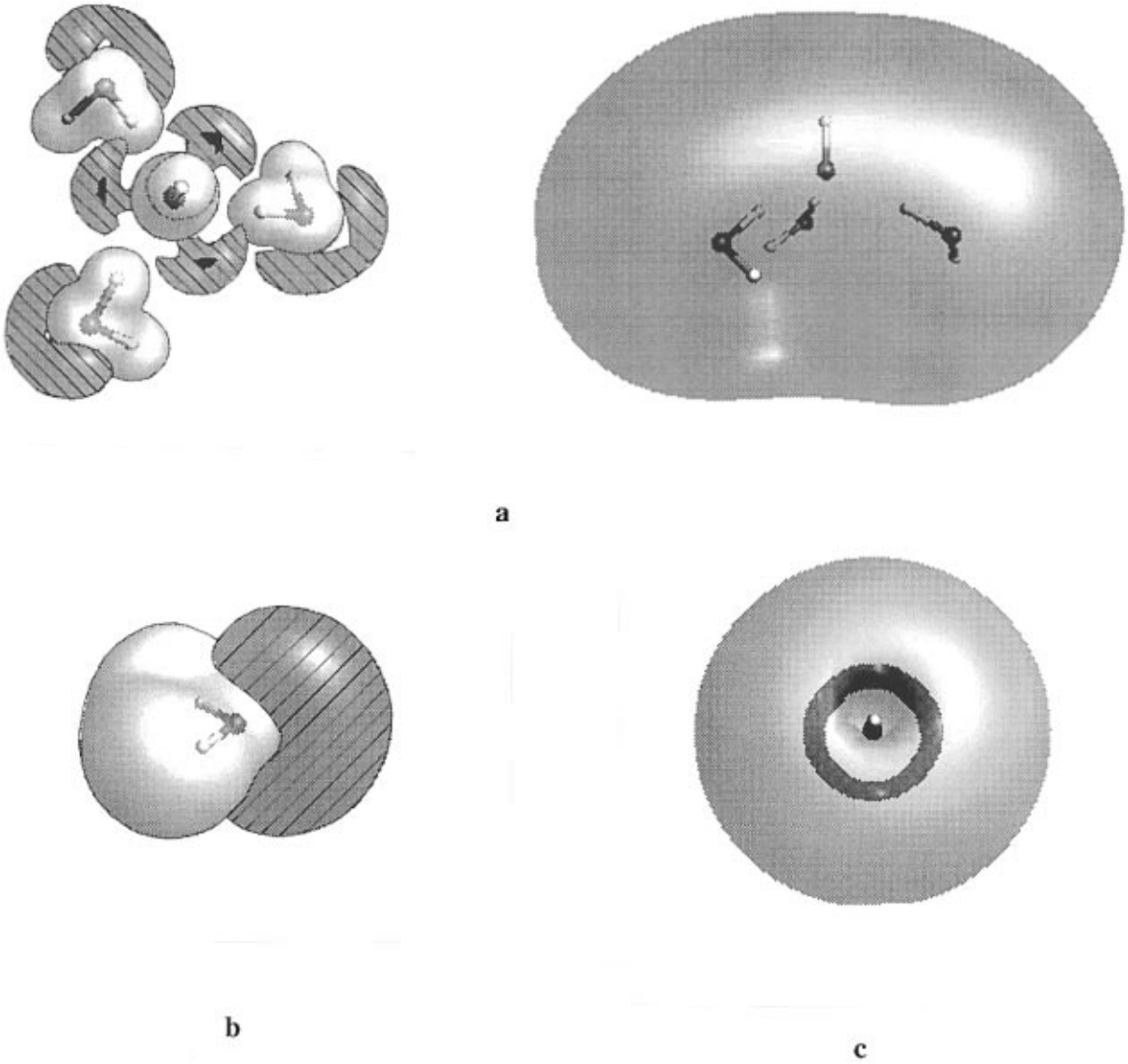

Figure 1. Molecular electrostatic potential maps computed using the BLYP method and the 6-31+G(2d,2p) basis set for (a, left) the $OH^-(H_2O)_3$ cluster, showing the region of potential −160 (dark), −140 (shaded), and 20 (light) kcal/mol, (a, right) the −60 kcal/mol region of the $OH^-(H_2O)_3$ cluster; (b) the H_2O molecule, showing the −20 (shaded) and 20 kcal/mol (light) regions, and (c) the OH^- anion (dark −240 kcal/mol region; light −110 kcal/mol region; the positive region, not shown for simplicity, is within the −240 surface, closer to the atoms).

idea of the most favorable orientations by looking at the relative orientations in which the positive regions of the molecular electrostatic potential (MEP) map[40] of one fragment overlaps the negative regions of the MEP map of the other fragment. The overlap of regions of opposite sign corresponds to attractive conformations. Among all the attractive orientations, the most stable ones are when the overlap is with the most negative regions, for a given positive potential. One should keep in mind that close to each nucleus there is always a positive region, as the electrostatic potential is infinite over the nucleus; positive regions are associated with zones where the electron density is depleted, and negative regions to zones where the electron density is high.

Figure 1a shows an upper and lateral view of the MEP map of the $OH^-(H_2O)_3$ cluster. The most negative regions of the MEP for this cluster are these between the three $H_{water}\cdots O_{OH^-}$ contacts (dark areas in Figure 1a), with a value of −160 kcal/mol. In these regions, a positive charge is more stable than in the shaded regions located on the lone pair regions of the water molecules (whose energy is −140 kcal/mol) or around the dark regions of the OH^- fragment. The MEP for the neutral water molecule is less negative, in consonance with the negative charge of the $OH^-(H_2O)_3$ cluster. Shown in Figure 1b is the volume of the −20 kcal/mol potential. Within that volume lies the minimum of the MEP, with a value of −62 kcal/mol, located in the region of the oxygen lone pairs. It is interesting to realize that the MEP map of the $OH^-(H_2O)_3$ cluster at large distance is negative, even in the OH^- hydrogen region; that is, it is not very different in shape from the MEP map of the isolated OH^- anion (Figure 1c). This fact will be important to understand the interacting properties of a water and the $OH^-(H_2O)_3$ cluster in the OH^- hydrogen region.

The overlap of the positive and negative regions of the $OH^-(H_2O)_3$ and H_2O MEP maps allows one to predict initial stable orientations for the $OH^-(H_2O)_3\cdots H_2O$ dimer. Among the various options, we have selected the following ones as most interesting. The first one, expectedly the most stable one, results after overlapping the positive region of the water molecule with the dark areas of the $OH^-(H_2O)_3$ cluster, thus giving rise to a tetrasolvated OH^- anion. The second possibility is the one in which the positive region of the isolated water molecule overlaps the negative regions of the first solvation waters of the $OH^-(H_2O)_3$ cluster; that is, the OH^- anion is trisolvated and the fourth water starts the second solvation shell. The third

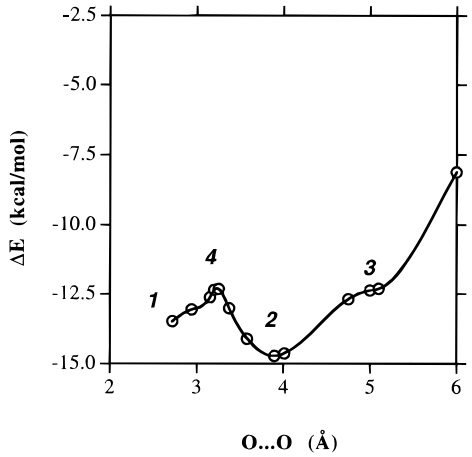

Figure 2. Variation of the interaction energy of the $OH^-(H_2O)_3\cdots H_2O$ cluster in its various conformations as a function of the O···O distance between the (OH^-) oxygen and the oxygen of the entering water.

option is obtained overlapping the negative potential of the isolated water with the positive regions of the waters of the cluster, giving rise to a cluster similar to the one obtained in the second option, but with the water acting as a proton acceptor. Finally, the fourth possibility is one in which the positive potential of the isolated water overlaps the negative regions of the OH^- fragment of the cluster in the region of the OH^- hydrogen. One should notice here that the previous MEP overlap analysis just discriminates between attractive and repulsive orientations and does not indicate if one orientation is a local minimum. The aggregate may show no local minimum for a relative orientation because it can distort toward another orientation which is energetically more favorable.

Full geometry optimizations started from the four conformers defined above were carried out at the BLYP/6-31+G(2d,2p) level. They ended in just two stationary conformations, hereafter identified as structures **1** and **2,** a tetrasolvated and trisolvated conformation, respectively. To investigate if there are other minimum energy structures in this region of the potential energy surface, we also studied the energetics of the $OH^-(H_2O)_3\cdots H_2O$ system as a function of the O···O distance, the distance between the oxygen of the OH^- and the oxygen of the water interacting with the $OH^-(H_2O)_3$ cluster. This search does not discard the presence of other minima in regions far from the one of interest here, as for instance those in which the OH^- anion is less than trisolvated in the surface of the cluster.

The search, carried out at the BLYP/6-31+G(2d,2p) level, was started at structure **1**, the one with the shortest O···O distance, and went out up to dissociation. Along this search, the O···O was fixed in each point and the internal geometry of the $OH^-(H_2O)_3$ and H_2O fragments was allowed to relax. The interaction energy obtained along the search is shown in Figure 2, while Figure 3 shows the geometry of the characteristic points **1**, **2**, **3**, and **4** marked on that energy curve, the first two corresponding to structures **1**, and **2**, while the last two are two new structures identified as **3** and **4**. The solid lines in Figure 3 identify the *only* intermolecular bonds found in the topological analysis of each conformer (see below). Let's have a look at these four characteristic structures in detail.

At the BLYP/6-31+G(2d,2p) level, structure **1** is a tetrasolvated OH^- anion with nearly C_{4v} symmetry. A vibrational analysis indicated that this conformer is a true minimum energy point, its interaction energy being −13.48 kcal/mol. The main parameters for the optimum geometry and energy of structure **1** are collected in Table 1. This structure is a stable conformer of the $OH^-(H_2O)_4$ cluster with solvation number equal to *four*,

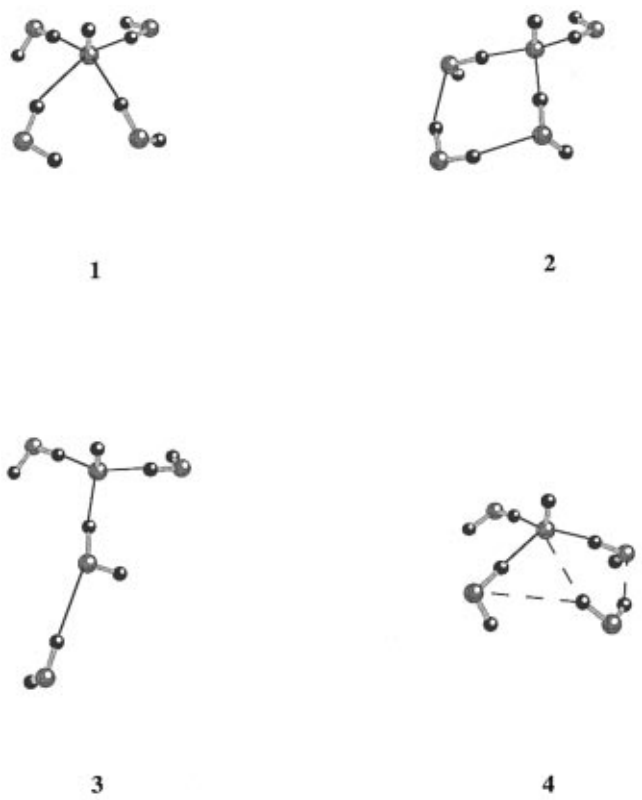

Figure 3. Structure of the $OH^-(H_2O)_3\cdots H_2O$ conformations in the characteristic points 1, 2, 3, and 4.

with the four waters directly attached to the oxygen OH^- atom. Therefore, *it breaks the commonly accepted idea that the maximum number of solvent molecules that an oxygen atom can accept is equal to the number of its lone pair electrons*, three in the OH^- case.

The existence of a tetrasolvated minimum energy conformer for the $OH^-(H_2O)_4$ cluster could be an artifact of the use of the BLYP method. Therefore, to discard that possibility, we repeated the full optimization of structure **1** at the MP2/6-31+G-(2d,2p) level, a method and basis set which is known to give good results for the geometry and stability of hydrogen bond systems.[41−43] The computations, started at the BLYP/6-31+G-(2d,2p) minimum energy, gave a final MP2 optimum geometry similar to the BLYP geometry, once again with four waters directly attached to the OH^- oxygen atom. Therefore, structure **1** is not an artifact of the BLYP methodology.

In structure **2**, the fourth water molecule is attached to two of the waters of the $OH^-(H_2O)_3$ cluster, thus starting the second solvation shell (see Figure 3). Full optimization of its geometry (see Table 1 for the optimum geometry and energy) gives a minimum energy point 14.72 kcal/mol below that of the $OH^-(H_2O)_3$ and H_2O fragments, and 1.24 kcal/mol below that for structure **1**. A vibrational analysis of the fully optimized geometry of structure **2** confirmed its true minimum energy nature.

Connecting structures **1** and **2** lies a maximum energy region (see Figure 2). A transition state, fully characterized by a vibrational analysis, is found in this region (structure **4** of Figure 3, where the broken lines indicate the bonds being formed and broken). Its energy lies 2.41 kcal/mol above that for structure **2** and 1.16 above that for structure **1**. These barriers are well within the range of thermally accessible energies at room temperature, and consequently, one should expect to find both conformers in the $OH^-(H_2O_4)$ clusters at room temperature.

As one enlarges the O···O contact in structure **2**, one of the two hydrogen bonds, the one linking the second solvation shell

TABLE 1: Optimum Energy (in Atomic Units), Minimum and Maximum Distance between the OH^- Oxygen Atom and the First Shell Molecules Attached to It ($r_{H\cdots O\ min}$ and $r_{H\cdots O\ max}$, Respectively, Both in Angstroms), and the Net Charge on the OH^- Hydrogen and Oxygen Atoms Computed by a Mulliken Population Analysis (q_H and q_O, Respectively, Both in Atomic Units) for the Optimum Geometry of $OH^-\cdots(H_2O)_n$ Clusters Computed at the BLYP/6-31+G(2d,2p) Level. The Number of Contacts with the Same Value of the Distance Is Indicated in Parentheses after the Distance

cluster	total energy	$r_{H\cdots O\ min}$	$r_{H\cdots O\ max}$	q_H	q_O
OH^-	−75.798 175			0.100	−1.100
H_2O	−76.423 667				
$OH^-\cdots(H_2O)_3$	−305.178 617	1.625 (3)		0.158	−0.967
$OH^-\cdots(H_2O)_4$ structure **1**	−381.623 770	1.707 (2)	1.734 (2)	0.167	−0.977
$OH^-\cdots(H_2O)_4$ structure **2**[a]	−381.625 747	1.588 (2)	1.648 (1)	0.165	−0.959
$OH^-\cdots(H_2O)_4$ structure **2**[b]	−381.624 732	1.569 (2)	1.777 (1)	0.164	−0.986
$OH^-\cdots(H_2O)_4$ structure **3**	−381.625 453	1.632 (2)	1.657 (1)	0.164	−0.983
$OH^-\cdots(H_2O)_4$ structure **4**	−381.621 912	1.563 (1)	2.495 (1)	0.164	−0.977
$OH^-\cdots(H_2O)_5$ structure **5**	−458.062 401	1.840 (5)		0.175	−0.978
$OH^-\cdots(H_2O)_5$ structure **6**	−458.068 044	1.670 (2)	1.745 (2)	0.174	−0.973
$OH^-\cdots(H_2O)_5$ structure **7**	−458.069 612	1.582 (1)	1.598 (2)	0.174	−0.954
$OH^-\cdots(H_2O)_6$ structure **8**	−534.508 429	1.561 (3)		0.162	−0.995

[a] Isomer shown in Figure 3b. [b] Isomer with an extra hydrogen bond, depicted in Figure 5.

water and two of the first solvation shell waters, is broken. Energetically, one reaches a small plateau because small changes in the O···O distance induce large variations in the O···O−H angle, the energetic change being small (see Figure 2). Structure **3** is the cluster conformation of this region, in which the $O_{OH-}\cdots O_{water}$−H angle is equal to zero. A vibrational analysis of structure **3** (optimized with the only restriction being that the $O_{OH-}\cdots O_{water}$−H bond should be collinear) gives very small positive values for the smallest eigenvalues of the Hessian matrix. However, one cannot consider structure **3** as a minimum because any small angular geometrical distortion gives rise to structure **2**, and consequently, it will not be stable against that distortion when the vibrational motion is accounted for. Finally, as the O···O distance in structure **3** is further increased, the interaction energy continuously decreases in a smooth way, until it reaches the zero limit.

The previous interaction energies are not corrected by the basis set superposition error (BSSE) that the use of truncated basis sets is introducing in our computations. Such error can be estimated for the interaction energy of the cluster relative to the $OH^-(H_2O)_3$ and H_2O fragments using the full-counterpoise method.[44] It is 0.57, 0.60, and 0.70 kcal/mol, for structures **1**, **2**, and **3**, respectively. Therefore, the shape of the surface does not change significantly by the inclusion of the BSSE corrections. This is not surprising in light of our previous studies on the size of the BSSE for hydrogen-bonded interaction energies computed using density functionals.[43] These studies showed that the BSSE was small for hydrogen-bonded dimers if a double-ζ plus diffuse plus double polarization basis set was used, as in our case. Therefore, we will not perform any more BSSE evaluations for the other clusters studied here giving its hydrogen-bonded nature.

We can center our attention now on the intermolecular contacts present in structures **1**−**3**. As we have pointed above, we have indicated by solid lines the *only* intermolecular contacts for which a bond critical point is found, that is, the only hydrogen bonds present in these structures. The density on these critical points lies around 0.025 au, that is, in the normal range found for critical points of hydrogen bond contacts.[37] In the three structures considered here one always finds hydrogen bonds connecting the OH^- fragment and the waters directly attached to it. However, no hydrogen bonds are found between any pair of waters in the first solvation shell of structures **1**−**3**. This was unexpected, given the orientation that shows the hydrogens of the first solvation shell waters toward the oxygens of the adjacent waters. It clearly shows the importance of performing a critical point analysis to properly characterize the nature of the intermolecular interactions present in complex molecular aggregates.

Figure 4. Optimum geometry structure of the $OH^-(H_2O)_3$ cluster and the $(H_2O)_2$ dimer. The intermolecular bonds found in the critical point analysis are indicated by solid lines.

Why are no hydrogen bonds present among the adjacent waters of the first solvation shell? If one looks at the shortest H···O distance between the waters of the first solvation shell (2.817 Å in structure **1** and 4.212 Å in structure **2**), one finds it larger than the optimum distance for the $(H_2O)_2$ dimer (2.078 Å). However, in the $(H_2O)_2$ dimer one finds critical points even when the shortest H···O distance is 4.212 Å. Therefore, the reason for the absence of a critical point in the first solvation shell of structures **1**−**3** has to be associated not with the distance but with the relative orientation of the adjacent waters. In effect, the interaction energy of a pair of adjacent waters of the first solvation shell of structure **1** is repulsive by 0.35 kcal/mol (BLYP/6-31+G(2d,2p) computation), and we cannot speak any more of the presence of a stable hydrogen bond. Therefore, the orientation of the waters in the first solvation shell is probably associated with long-range electrostatic effects between the adjacent waters, or between the waters and the OH^- fragment (notice that the dangling OH groups of the first shell waters point to the position in which the MEP maps present their most negative regions). The situation is similar to the interaction between the methyl groups of the ethylene molecule, responsible for the rotational barrier in that molecule.

We have also carried out a critical point search on the optimum structure of the $OH^-(H_2O)_3$ cluster and the $(H_2O)_2$ dimer, both optimized at the BLYP/6-31+G(2d,2p) level (see Figure 4 for the optimum geometries, where solid lines indicate the only hydrogen bonds). In the $OH^-(H_2O)_3$ case, the shortest H···O distance between the first shell waters is 3.787 Å, again much longer than the one in the $(H_2O)_2$ dimer (2.078 Å). The critical point analysis of the $OH^-(H_2O)_3$ cluster shows the presence of (3,−1) bond critical points between the shortest H···O contacts of the three waters and the OH^- fragment but not between any of the three waters. A bond critical point is

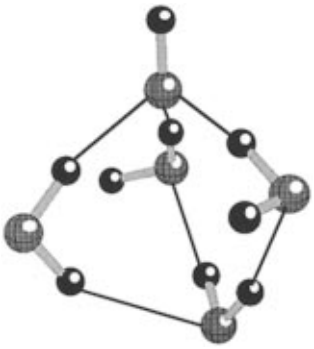

Figure 5. Optimum geometry structure of the high-energy conformer for the $OH^-(H_2O)_4$ cluster. The intermolecular bonds found in the critical point analysis are indicated by solid lines.

found for the shortest H···O distance of the $(H_2O)_2$ dimer, the only hydrogen bond one expects for this dimer. Notice that the preference of this dimer for a trans conformation comes from the long-range H···H contacts, which are necessarily Coulombic, as no critical points are present between them. All of this confirms the validity of the analysis carried out on structures **1**−**3** regarding the absence of water···water hydrogen bonds in the first solvation shell of these structures.

In our search for all the minimum energy conformations of the $OH^-(H_2O)_4$ cluster we have also found a second minimum (see Figure 5) for structure **2**, which lies 0.64 kcal/mol above the energy of the first conformer of the same structure (Figure 3). Both structures are similar. The new conformer is more compact and shows a new hydrogen bond (between the second solvation shell water and the first shell water that was not solvated to it in the Figure 3 conformer). The formation of the new hydrogen bond is confirmed by a topological analysis of the electron density. A vibrational analysis of the optimum structure of the new conformer shows that it is a true minimum energy point. The lower stability for the new conformer is an indication of the superior strain of its geometry. We did not try to locate the transition state between the two conformers.

As mentioned in the Introduction, the energetics of the water approaching the $OH^-(H_2O)_3$ cluster along the direction of the OH^- hydrogen region is very important for a better understanding of the possible water rearrangements which can take place in that region upon the formation of the OH^- anion from the XOH molecule. Qualitatively, the reason for the rearrangement can be easily understood comparing the MEP maps of the OH^- anion and an isolated water molecule in the OH^- hydrogen region (see Figure 1 for both MEP maps): positive regions in the isolated water become negative in the OH^- anion. Therefore, while attaching a water in that region was stable (see the optimum geometry of the water dimer in Figure 4), it will become less stable or even unstable after the proton is transferred.

The interaction energy of a water attached to the $OH^-(H_2O)_3$ cluster in the OH^- hydrogen region was computed looking at the energy of the $OH^-(H_2O)_3\cdots H_2O$ system as a function of the parameters r and α forcing the water oxygen to be collinear with the OH^- axis. The first parameter is the O···O distance between the oxygen of the interacting water and the OH^- oxygen of the $OH^-(H_2O)_3$ cluster. The angle α is that formed by the coaxial axis of the OH^- anion and the C_{2v} axis of the attaching water. The $OH^-(H_2O)_3$ cluster was taken in its most stable geometry (Figure 4, Table 1) at the BLYP/6-31+G(2d,-2p) level. The attaching water geometry is its optimum BLYP/6-31+G(2d,2p) one. Both fragments were kept frozen during the computation of the $E(r,\alpha)$ potential map. Figure 6 shows the $E(r,\alpha)$ map obtained at the BLYP/6-31+G(2d,2p) level. The

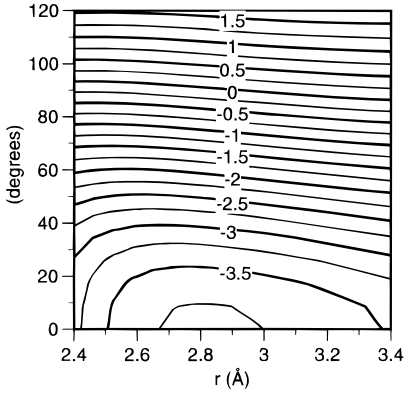

Figure 6. Potential energy surface as a function of the O···O distance (r) and the angle between the water C_{2v} axis and the OH^- axis (see text).

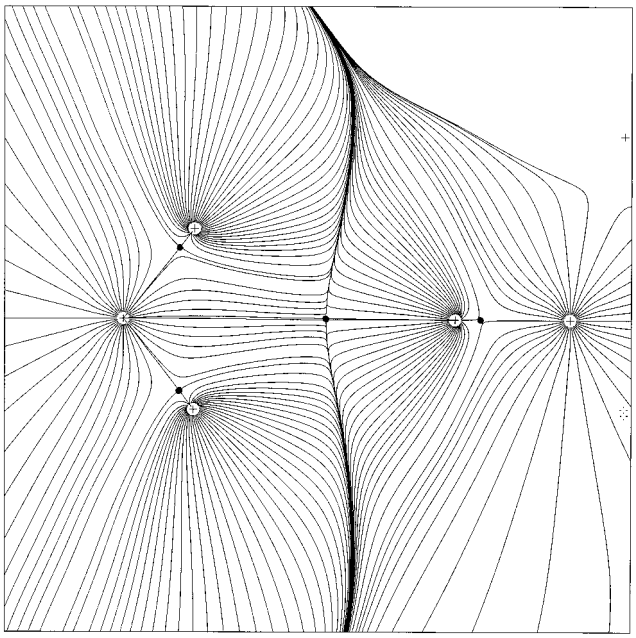

Figure 7. Map of the gradient vector field of the electron density ($\nabla\rho(r)$)in the region of the OH^- hydrogen atom, showing the critical points in the water and OH^- fragments, and also between these two fragments. Each line represents a trajectory of $\nabla\rho(r)$.

map is attractive for $\alpha < 90°$, its lowest energy being the one for $\alpha = 0°$ and $r \cong 2.8$ Å. Therefore, attaching a water to the $OH^-(H_2O)_3$ cluster in the OH^- hydrogen region is a stable process if the water hydrogens point to the OH^- hydrogen, in good agreement with the conclusions from a MEP overlap analysis (see Figure 1). The attachment becomes repulsive when the oxygen of the water points to the OH^- hydrogen (Figure 3) at $\alpha > 90°$. Identical conclusions are reached if the fragment's geometry is fully optimized and a cut on the surface is performed. A critical point analysis of the cluster with the water oriented at $\alpha = 0°$ and $r \cong 2.8$ Å shows the presence of a hydrogen bond between the OH^- hydrogen and the water attached to it. This is shown in Figure 7, which represents the gradient of the density in the region of the $OH^-\cdots$water critical point. One finds three critical points: two for the O−H bonds of the water, one for the O−H bond in the OH^- anion, and the $OH^-\cdots$water critical point in the middle. Notice that in the $OH^-\cdots$water critical point the contact is established between the OH^- hydrogen and the water oxygen. Therefore, according to this analysis, the $OH^-\cdots$O intermolecular bond is preserved when the OH^- fragment is formed. This bond is about 3.8 kcal/mol strong, according to our BLYP/6-31+G(2d,2p) computa-

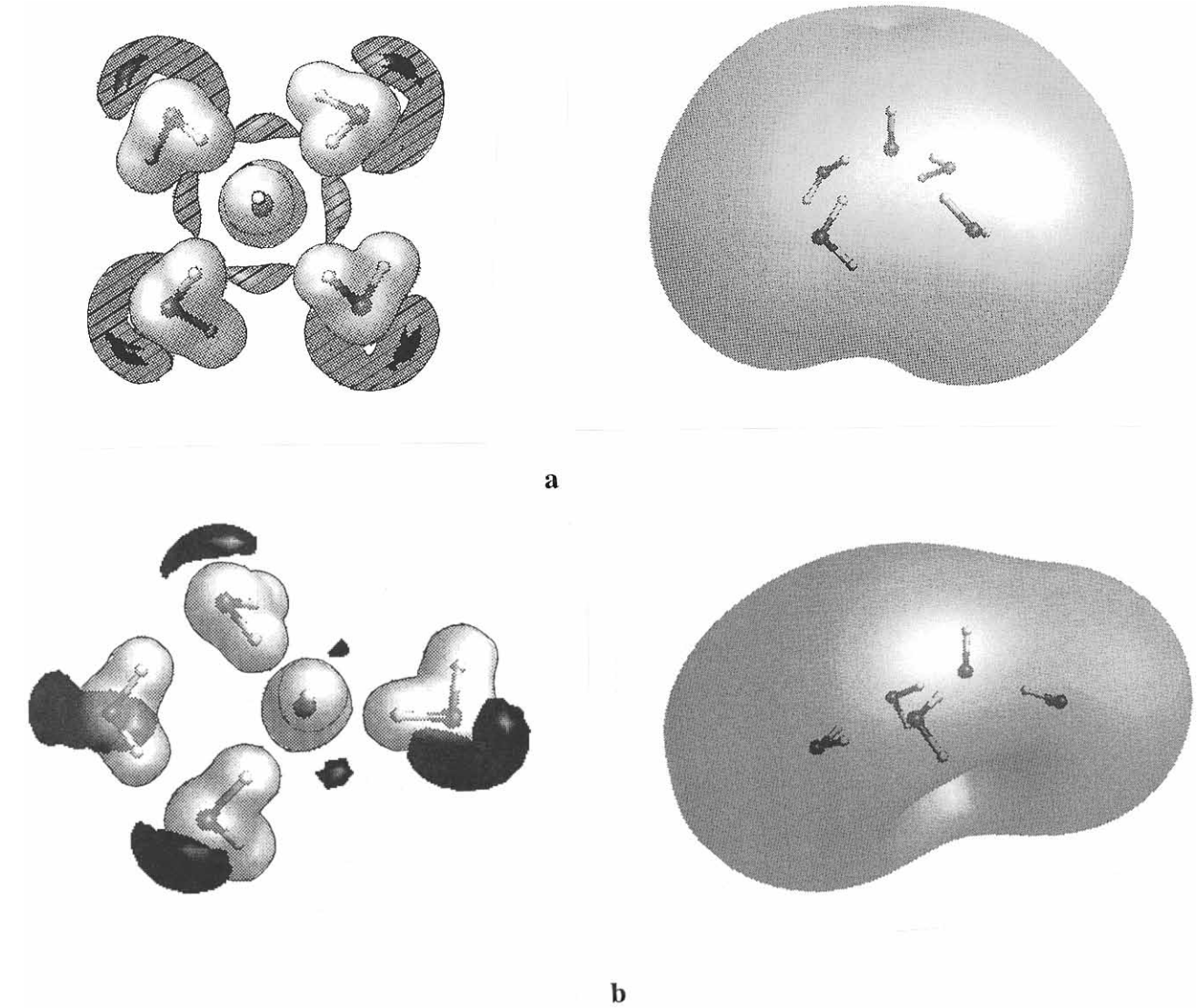

Figure 8. Molecular electrostatic potential maps computed using the BLYP method and the 6-31+G(2d,2p) basis set for the two conformers of the $OH^-(H_2O)_4$ cluster: (a) structure **1**, upper view (−135 kcal/mol, light 20) and side view (light −60 kcal/mol); (b) structure **2**, upper view (dark −140 kcal/mol, shaded −130, light 20) and side view (light −60 kcal/mol).

tions, which can be compared with the 4.59 kcal/mol required to break the hydrogen bond in the water dimer at the same computational level. The weaker nature of the $OH^-\cdots O$ intermolecular bond in the $OH^-(H_2O)_3\cdots H_2O$ system compared to the $OH\cdots O$ bond of the $(H_2O)_2$ dimer is also manifested in the smaller density in the critical point of the first bond (just 0.005 au, compared to the 0.02 au value in the later).

The $E(r,\alpha)$ map also gives a quantitative idea of the size of the force involved in the water rearrangement in the $OH^-(H_2O)_3$ cluster case: a water attached to the OH^- and oriented along the direction of the lone pair electrons at a distance of 2.5 Å is repulsive by about 1.5 kcal/mol, nearly 5 kcal/mol above the optimum conformation for a water attached to the OH^- hydrogen found in Figure 6. By twisting its hydrogens, it gains enough energy to fully break one hydrogen bond or partially break some others.

Finally, although Figure 6 shows that a water is stable attached to the OH^- hydrogen, there is no real minimum energy point in this region when all degrees of freedom are left free, in good agreement with other studies.[21] All the full geometry optimization started from a point in the low-energy region of Figure 6 ended in structure **2**. We explored the cause for this behavior by computing the optimum energy for the $OH^-(H_2O)_3\cdots H_2O$ system as a function of the angle formed by the oxygen of the entering water and the axis of the OH^- anion, hereafter called β. When $\beta = 180°$, the collinear situation, the energy curve is nearly flat and has the shape of a maximum. As β decreases, the interaction energy also decreases, first slowly up to $\beta = 165°$ and then sharply as we move away from that value. This can be rationalized looking at the MEP map of the cluster: the region around the OH^- hydrogen is a lot less negative than the one around the first solvation shell waters. The shift along β implies the breaking of the weaker $OH^-\cdots$water hydrogen bond and the formation of a stronger water$\cdots$water bond (see above for estimates of these bond strengths). Each of these hydrogen bonds has one diabatic associated to it. The drift of a water along β is like a reaction in which the reactant is a lot less stable than the product. In terms of diabatics, it is well-known that when the diabatics for reactants and products show a very different stability, there is no barrier for the reaction in the adiabatic, because the two diabatics intersect around the diabatics minimum. Therefore, *the lack of minimum energy conformations when a water is attached to the OH^- hydrogen is a consequence of the much lower stability of this conformer compared to the case in which the same water gets attached to the equatorial waters*. Notice that the lateral shift of the water along β can be avoided if that water is linked to other waters also attached to the equatorial

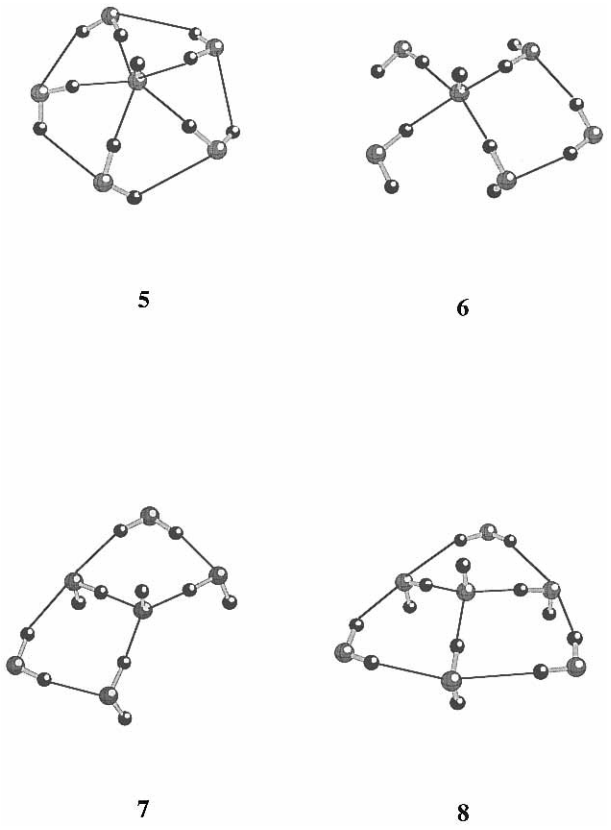

Figure 9. Optimum geometry for the minimum energy structures **5**, **6**, and **7** of the $OH^-(H_2O)_5$ cluster. The intermolecular bonds found in the critical point analysis are indicated by solid lines.

ones; that is, the shift should not be present in large enough $OH^-(H_2O)_n$ clusters or in solids.

Structure and Stability of the $OH^-(H_2O)_5$ Cluster. One can repeat the procedure employed above in the $OH^-(H_2O)_4$ cluster on the $OH^-(H_2O)_5$ cluster and thus systematically locate all the possible minimum energy structures of the $OH^-(H_2O)_5$ cluster by looking at the energetics for the addition of a water to the $OH^-(H_2O)_4$ cluster. There are two possible conformers with similar stability for the $OH^-(H_2O)_4$ cluster, structures **1** and **2**. Therefore, we should look at the MEP maps of these two structures (Figure 8) and carry out a MEP overlap analysis with the MEP map of the isolated water to locate the expected regions where the addition of a water is more stable.

The MEP map for structure **1** shows its more negative region located on the oxygen atoms of the first solvation shell waters. This region is a bit more energetic than the region close to the OH^- oxygen. The OH^- hydrogen region is, once again, a weakly negative region. A simple qualitative MEP overlap analysis suggests three possible structures for the new $OH^-(H_2O)_5$ cluster: (a) a first one with a water attached to any of the four first solvation waters, (b) a second one with five waters directly attached to the OH^- oxygen, and (c) a third one with a water attached to the OH^- hydrogen. Given the similarity between the $OH^-(H_2O)_3$ and $OH^-(H_2O)_4$ MEP map in the OH^- hydrogen region, we do not expect the water to be a minimum energy geometry in the third conformation. Such a fact was confirmed by a full BLYP/6-31+G(2d,2p) geometry optimization (see below). Concerning the a and b approximations, full BLYP/6-31+G(2d,2p) geometry optimizations ended in structures **5** and **6** (see Figure 9). The first one is the result of adding a fifth water to the OH^- oxygen of structure **1** in a pentagonal arrangement, while the second one is the result of the adding a new second shell water to the first solvation shell of structure **1**. The energy of structure **5** lies 3.54 kcal/mol above that for structure **6**, in good agreement with the expectations from our MEP overlap analysis. A vibrational analysis of the two structures demonstrates that both are true minimum energy points. Little distortions of structure **5** easily ended in structure **6**, a clear indication that the barrier separating these two conformers was very small and very close to the optimum geometry of structure **5**. In any case, structure **5** shows that in principle a pentasolvation of the OH^- oxygen, is possible although not energetically very stable. The critical point analysis of the optimum geometry of structure **5** shows the presence of critical points between the five first solvation waters. These critical points have a smaller density than the ones found between the five waters and the OH^- anion (0.008 au, compared to 0.035 au). The H···O distance for the low-density critical points of structure **5** is 2.539 Å, that is, a lot shorter than the equivalent distances in structure **1**. By comparison, the critical point analysis of structure **6** (Figure 9) shows only the presence of intermolecular bond critical points between the newly added water and the first solvation shell waters and between these and the OH^- anion.

Once the possibilities of adding a water to structure **1** of the $OH^-(H_2O)_4$ cluster have been analyzed, we can repeat the analysis starting from structure **2**. The MEP map of this second conformer is shown in Figure 8. Its most negative region is located on the water oxygens, without distinction of first or second solvation shells. It also has a little less stable region located on the OH^- oxygen. Consequently, a new water molecule will have a strong preference to be attached to the lone pairs of any of the waters of the $OH^-(H_2O)_4$ cluster or to the OH^- anion. In the first case, the resulting cluster is structure **7**, while in the second one, the final product is structure **6**. There is an interconversion between these two structures, similar to the one found above for structures **1** and **2**. Consequently, given their similar energetic stability (structure **7** is just 0.98 kcal/mol more stable, see Table 1) one should expect the presence of both conformers with similar probability at room temperature. Structure **7** is similar to the structure of the $OH^-(H_2O)_6$ cluster in its hexagonal conformation (structure **8** in Figure 8), but without one water molecule. There is also other possible conformer for a $OH^-(H_2O)_5$ cluster obtained by adding the new water to the second solvation shell water, thus starting the third solvation shell. As this possibility is not interesting to understand the structure of the first solvation shell of the OH^- anion, we did not further investigate its properties.

As mentioned before, we have also explored the stability of a water attached to the OH^- hydrogen of the $OH^-(H_2O)_4$ cluster. At the BLYP/6-31+G(2d,2p) level, a full geometry optimization of a $OH^-(H_2O)_5$ cluster built by adding a new water to structure **1** (see Figure 3) with the water lone pair electrons pointing to the OH^- hydrogen and at an H···O distance of 2.3 Å, ended in structure **6**. Equivalent results were obtained starting from structure **2**. However, although no minimum energy conformation is found, we found that the water is energetically stable against its dissociation in this region, when its hydrogens point toward the OH^- hydrogen. The result is similar to the one indicated above for the $OH^-(H_2O)_4$ cluster, not surprisingly given the similarity in the MEP maps in the OH^- region of the involved clusters. Consequently, the recent report[22] indicating the presence of minimum energy conformers of $OH^-(H_2O)_5$ clusters within a $OH^-(H_2O)_{31}$ cluster in which one water was attached to the OH^- hydrogen has to be a consequence of the influence of the extra waters surrounding the $OH^-(H_2O)_5$, which impose restrictions on the displacements of the water molecule attached to the OH^- hydrogen. We will fully demonstrate this affirmation in the following section.

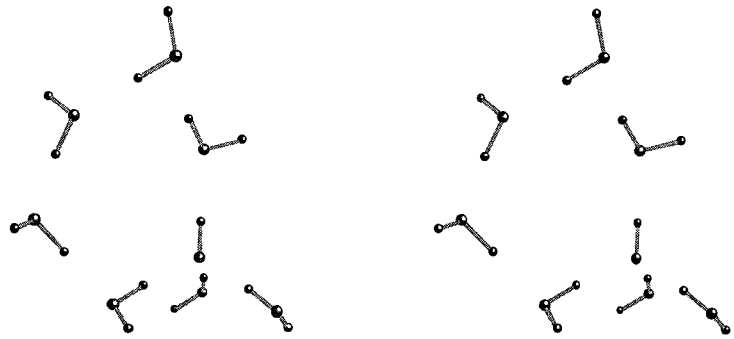

$OH^-(H_2O)_7$

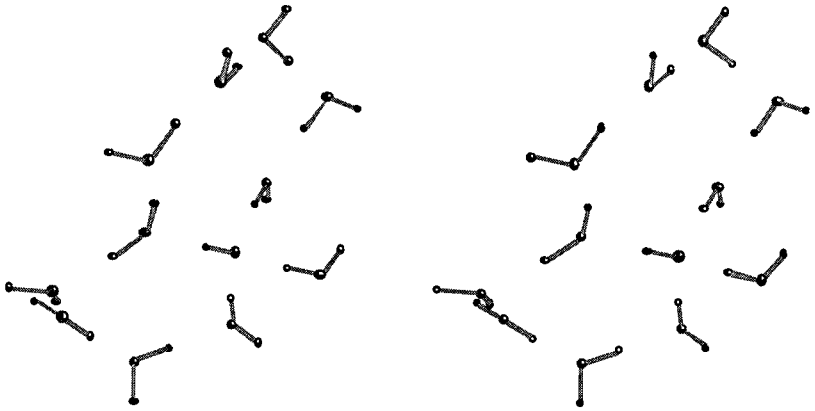

$OH^-(H_2O)_{11}$

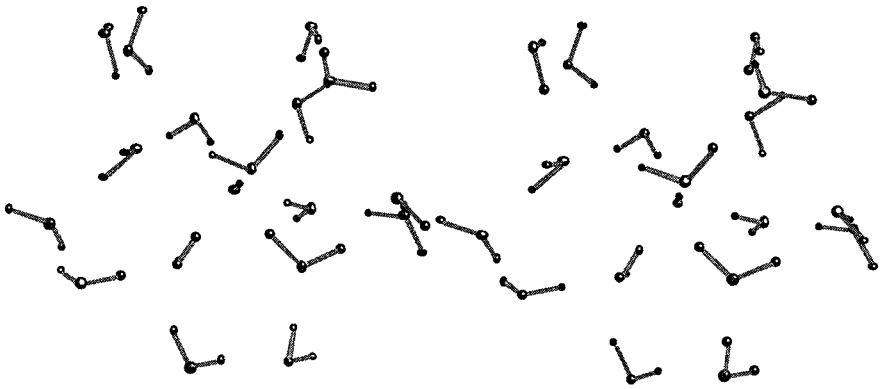

$OH^-(H_2O)_{17}$

Figure 10. Stereoview of the initial geometries of the $OH^-(H_2O)_7$, $OH^-(H_2O)_{11}$, and $OH^-(H_2O)_{17}$ clusters.

Higher Hydrated $OH^-(H_2O)_n$ Clusters. Understanding at the molecular level the exact details of the mechanisms of the possible water rearrangement is only possible if one has minimum energy conformations for the $OH^-(H_2O)_n$ clusters in which some waters lie in the OH^- hydrogen region. As seen above, an isolated water molecule attached to the OH^- hydrogen

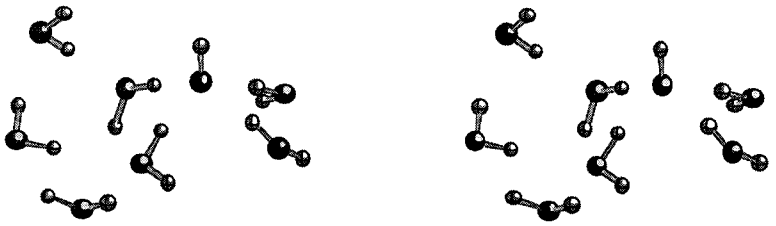

$OH^-(H_2O)_7$

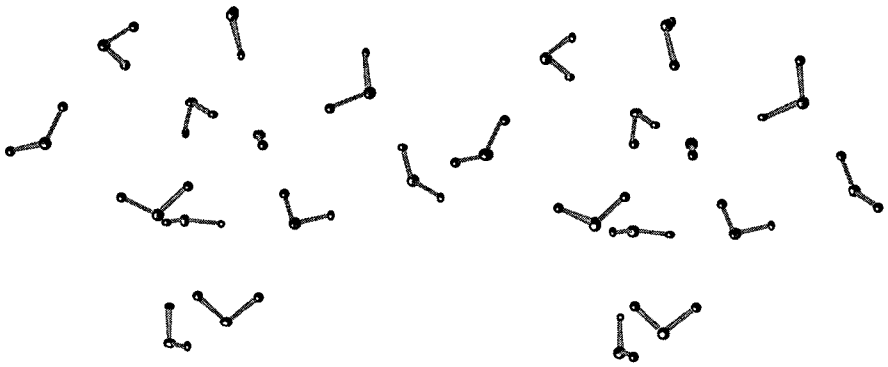

$OH^-(H_2O)_{11}$

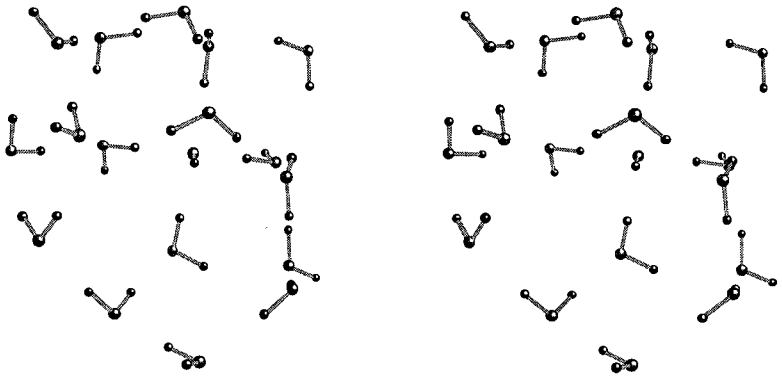

$OH^-(H_2O)_{17}$

Figure 11. Stereoview of the final optimized geometries of the $OH^-(H_2O)_7$, $OH^-(H_2O)_{11}$, and $OH^-(H_2O)_{17}$ clusters.

of the $OH^-(H_2O)_4$ and $OH^-(H_2O)_5$ clusters drifts toward the first solvation shell of waters attached to the OH^- oxygen. If other waters are present around these in the $OH^-(H_2O)_5$ cluster, that shift could be partially or totally avoided by the surrounding waters. These surrounding waters create a network of hydrogen bonds which the drifting molecule has to break or at least strongly distort in order to move. Recent dynamical studies on $OH^-(H_2O)_{31}$ clusters[22] seem to indicate that the drift is

Figure 12. Stereoview of the region of the $OH^-(H_2O)_{17}$ cluster in which the $OH^-\cdots O$ critical point is located, showing the critical point.

avoided in such a large cluster. In this section, we will show that this is not a consequence of the dynamical methodology, but a consequence of the hydrogen bonds connecting the $OH^-(H_2O)_4$ and $OH^-(H_2O)_5$ fragments of the cluster with the surrounding water molecules. We will prove this idea by systematically building $n > 5$ clusters in which the OH^- hydrogen water is progressively more attached to the first solvation shell waters linked to the OH^- oxygens. By restricting all the possible drifts one can stabilize that water.

Our search for a $OH^-(H_2O)_n$ cluster having a minimum energy conformer in which a water is attached to the OH^- hydrogen started in the $OH^-(H_2O)_7$ cluster shown in Figure 10. This clusters was built by adding one water to the OH^- hydrogen of the three-coordinated form of the $OH^-(H_2O)_3$ cluster, linking this water to the equatorial ones by a chain of three water molecules. Why three waters in the link? Because this is the minimum number allowed to form the link without creating too much of a strain in the link, but larger links could also work. A full HF/6-31+G(2d,2p) geometry optimization of the initial $OH^-(H_2O)_7$ geometry (Figure 10) ended in a more stable structure showing no waters attached to OH^- hydrogen (see Figure 11). Instead the three waters added to the link and the OH^- hydrogen water have moved to maximize the contacts with the first solvation shell waters.

Looking at the optimization pathway followed by the geometrical optimization of the $OH^-(H_2O)_7$ cluster, we concluded that the structure did not have enough restrictions in the OH^- hydrogen region to avoid the drift toward the first solvation shell waters. Therefore, we increase the number of connections of the water attached to the OH^- hydrogen by adding a second chain of waters to the starting $OH^-(H_2O)_4$ structure, thus linking two sides of the OH^- hydrogen water to the first solvation shell waters. This second connection was established by a link of four waters. Therefore, the resulting cluster is the $OH^-(H_2O)_{11}$ cluster shown in Figure 10. When its geometry is fully optimized at the HF/6-31+G(2d,2p) level, once again the structure collapses into one with no water attached to the OH^- hydrogen (see Figure 11). Interestingly, the final geometry of the $OH^-(H_2O)_{11}$ cluster has a tetrasolvated OH^- fragment in it, similar to a distorted structure **1**, although the optimization was started with a trisolvated OH^- anion like structure **2**.

Trying to have a less flexible structure, we added more waters to attach the OH^- hydrogen water more rigidly and in a symmetric form. In this way we built the $OH^-(H_2O)_{17}$ cluster, whose initial structure is shown in Figure 10. The optimization of the geometry of this cluster at the HF/6-31+G(2d,2p) level gave a final optimized structure with waters in the region of the OH^- hydrogen (Figure 11). A critical point analysis of that cluster revealed that there is one $OH^-\cdots$water hydrogen bond between the OH^- hydrogen and one of the waters close to it. Figure 12 shows a stereoview of the $OH^-\cdots$water region, indicating the position of the critical point by a full circle. The OH^- hydrogen is 2.909 Å from the water oxygen, and the $O-H\cdots O_{water}$ angle is 133°, with the hydrogens of the water pointing to the OH^- hydrogen. So, we have been able to find a $OH^-(H_2O)_n$ cluster in which a water is hydrogen bonded to the OH^- hydrogen. This was done by creating enough links between this water and the rest of the waters of the rest of the cluster in a symmetrical form.

There is a striking similarity between the first solvation shell of the $OH^-(H_2O)_{17}$ cluster and that obtained in some of the ab initio molecular dynamics structures.[22] In both clusters one can find a distorted $OH^-(H_2O)_4$ fragment of the type found in structure **1**, in which the OH^- anion has five water molecules directly attached to it: four linked to the oxygen and one to the hydrogen. This makes the total coordination number of the OH^- anion equal to *five*. There is no reason to believe that this is the only possible structure for a $OH^-(H_2O)_{17}$ cluster having the same coordination number. On the other hand, one can have more than one coordination number for the OH^- anion in the $OH^-(H_2O)_{17}$ cluster: the $OH^-(H_2O)_4$ fragment of this cluster can present the equilibrium between the tetra- and three-coordinated OH^- oxygen conformers similar to that already described in structures **1** and **2**. The observed final average depends on the relative stability between the various types of conformers. We will not explore this point at this time, as our emphasis in this work was only to show the existence of minimum energy structures with solvation numbers larger than three and to understand the reasons for its stability.

Concluding Remarks

By doing BLYP/6-31+G(2d,2p) and HF/6-31+G(2d,2p) computations, we have been able to show the existence of conformers of the $OH^-(H_2O)_4$ and $OH^-(H_2O)_5$ clusters with four and five waters directly attached to the OH^- oxygen atom. The $OH^-(H_2O)_4$ conformer, with four solvated waters in the first shell, is 1.24 kcal/mol more stable than the trisolvated one. The transition state connecting these two conformers lies 2.41 kcal/mol above the trisolvated structure and 1.16 above the tetrasolvated one. Therefore, one should find both types of solvation at room temperature. On the other hand, the tetrasolvated structure of the $OH^-(H_2O)_5$ cluster is much more stable than the pentasolvated one, and the barrier separating them is negligible. So, the chances of finding pentasolvated OH^- oxygens in these clusters is very small.

We have also shown that attaching a water molecule to the OH^- hydrogen of the $OH^-(H_2O)_3$ and $OH^-(H_2O)_4$ clusters is energetically favorable when the two hydrogens point to the OH^- hydrogen. However, such conformation is not a minimum energy on the potential energy surface of these clusters. The reason is the much higher stability of the OH^- hydrogen water when it is attached to one of the first solvation shell waters of the $OH^-(H_2O)_3$ and $OH^-(H_2O)_4$ clusters.

We ended searching for structures in which the previous shift was avoided. This was done using more hydrated clusters which present waters linking the water attached to the OH^- hydrogen and the waters of the first solvation shell. In doing so, we have found a $OH^-(H_2O)_{17}$ cluster in which the drift is avoided. The initial geometry of this cluster has the water attached to the OH^- hydrogen simultaneously linked to three first solvation shell waters. The final optimum structure presents four waters coordinated to the OH^- through its oxygen and one more water coordinated to the OH^- hydrogen, thus making the total solvation number of this structure equal to five. It is also possible to have coordination numbers equal to four if the equilibrium between four and three waters coordinated to the OH^- oxygen found in the $OH^-(H_2O)_4$ cluster would hold for the $OH^-(H_2O)_4$ fragment present within the $OH^-(H_2O)_{17}$ cluster.

Acknowledgment. This work was supported by the DGCYT under Projects PB-92-0655-C02-02 and PB95-0848-C02-02 and by CIRIT under project GRQ94-1077, respectively. We also express our gratitude to CESCA/CEPBA for allocating computer time in their machines. The stay of C.P. in our laboratory was partially supported by the "Access to Supercomputing Facilities for European Researchers" project of the Training and Mobility of Researchers (program contract ERBFMGECT950062 (DG-12 MEMO)), established between the European Community and CESCA/CEPBA. M.P. thanks "Ministerio de Educacion y Ciencia" for his doctoral grant.

References and Notes

(1) Busing, W. R.; Horning, D. F. *J. Phys. Chem.* **1961**, *65*, 284.
(2) Giguère, P. A. *Rev. Chim. Miner.* **1983**, *20*, 588.
(3) Maiorov, V. D.; Bocharova, L. V.; Librovich, N. B. *Russ. J. Phys. Chem.* **1982**, *56*, 67. Librovich, N. B.; Maiorov, V. D. *Russ. J. Phys. Chem.* **1982**, *56*, 380.
(4) Moruzzi, J. L.; Phelps, A. V. *J. Chem. Phys.* **1966**, *45*, 4617.
(5) De Paz, M.; Giardini, A. G.; Friedman, L. *J. Chem. Phys.* **1970**, *52*, 687.
(6) Ashadi, M.; Kebarle, P. *J. Phys. Chem.* **1970**, *74*, 1483.
(7) Klots, C. E.; Compton, R. N. *J. Chem. Phys.* **1978**, *69*, 1644.
(8) Knapp, M.; Echt, O.; Kreisle, D.; Recknagel, E. *J. Chem. Phys.* **1986**, *85*, 636.
(9) Meot-Ner (Mautner), M.; Speller, C. V. *J. Phys. Chem.* **1986**, *90*, 6616.
(10) Yang, X.; Castleman, A. W., Jr. *J. Phys. Chem.* **1990**, *94*, 8500.
(11) Newton, M. D.; Ehrenson, S. *J. Am. Chem. Soc.* **1971**, *93*, 4971.
(12) Szczesniak, M. M.; Scheiner, S. *J. Chem. Phys.* **1982**, *77*, 4586.
(13) Sapse, A. M.; Osorio, L.; Snyder, G. *Int. J. Quantum Chem.* **1984**, *26*, 223.
(14) Ohta, K.; Morokuma, K. *J. Phys. Chem.* **1985**, *89*, 5845.
(15) Rohlfing, C. M.; Allen, L. C.; Cook, C. M.; Schlegel, H. B. *J. Chem. Phys.* **1983**, *78*, 2498.
(16) Andres, J. L.; Duran, M.; Lledos, A.; Bertran, J. *Chem. Phys. Lett.* **1986**, *124*, 177.
(17) Carbonell, E.; Andres, J. L.; Lledos, A.; Duran, M.; Bertran, J. *J. Am. Chem. Soc.* **1988**, *110*, 996.
(18) Del Bene, J. E. *J. Phys. Chem.* **1988**, *92*, 2874.
(19) Xantreas, S. S. *J. Am. Chem. Soc.* **1995**, *117*, 10373.
(20) Kendall, R. A.; Dunning, T. H., Jr. *J. Chem. Phys.* **1992**, *96*, 6796.
(21) Tuñon, I.; Rinaldi, D.; Ruiz-Lopez, M. F.; Rivail, J. L. *J. Phys. Chem.* **1995**, *99*, 3798.
(22) Tuckerman, M.; Laasonen, K.; Sprik, M.; Parrinello, M. *J. Phys. Chem.* **1995**, *99*, 5749.
(23) Eigen, M. *Angew. Chem., Int. Ed. Engl.* **1963**, *3*, 1.
(24) Albery, W. J. *Prog. React. Kinet.* **1967**, *4*, 353.
(25) Ando, K.; Hynes, J. T. *J. Mol. Liq.* **1995**, *64*, 25.
(26) Lee, C.; Sosa, C.; Novoa, J. J. *J. Chem. Phys.* **1995**, *103*, 4360.
(27) Lee, C.; Sosa, C.; Planas, M.; Novoa, J. J. *J. Chem. Phys.* **1996**, *104*, 7081.
(28) Planas, M.; Lee, C., Novoa, J. J. *J. Phys. Chem.* **1996**, *100*, 16495.
(29) Lee, C.; Fitzgerald, G.; Planas, M.; Novoa, J. J. *J. Phys. Chem.* **1996**, *100*, 7398.
(30) Parr, R. G.; Yang, W. *Density Functional Theory of Atoms and Molecules*; Oxford University Press: New York, 1989.
(31) ACS Symposium Series 629; Laird, B. B., Ross, R. B., Ziegler, T., Eds., Washington, DC, 1996.
(32) Becke, A. D. *Phys. Rev. A* **1988**, *38*, 3098.
(33) Lee, C.; Yang, W.; Parr, R. G. *Phys. Rev. B* **1993**, *37*, 785.
(34) Perez del Valle, C.; Planas, M.; Novoa, J. J. Chem. Phys. Lett., in press.
(35) Frisch, M. J.; Trucks, G. W.; Schlegel, H. B.; Gill, P. M. W.; Johnson, B. G.; Robb, M. A.; Cheeseman, J. R.; Keith, T.; Peterson, G. A.; Montgomery, J. A.; Raghavachari, K.; Al-Laham, M. A.; Zakrzewski, V. G.; Ortiz, J. V.; Foresman, J. B.; Ciolowski, J.; Stefanov, B. B.; Nanayakkara, A.; Challacombe, M.; Peng, C. Y.; Ayala, P. Y.; Chen, W.; Wong, M. W.; Andres, J. L.; Replogle, E. S.; Gomperts, R.; Martin, R. L.; Fox, D. J.; Binkley, J. S.; Defrees, D., J.; Baker, J.; Stewart, J. P.; Head-Gordon, M.; Gonzalez, C.; Pople, J. A. *Gaussian 94*, Revision C.3; Gaussian, Inc.: Pittsburgh, PA, 1995.
(36) Ditchfield, D.; Hehre, W. J.; Pople, J. A. *J. Chem. Phys.* **1971**, *54*, 724.
(37) Bader, R. F. W. *Atoms in Molecules. A Quantum Theory*; Clarendon Press: Oxford, 1994.
(38) Cioslowski, J.; Nanayakkara, A.; Challacombe, M. *Chem. Phys. Lett.* **1993**, *203*, 1993.
(39) Biegle-Köning, F.; Bader, R. F. W., Tang, W.-H. *J. Comput. Chem.* **1982**, *3*, 317.
(40) Scrocco, E.; Tomasi, J. *Adv. Quantum Chem.* **1978**, *11*, 115. Politzer, P.; Murray, J. S. *Rev. Comput. Chem.* **1991**, *2*, 273.
(41) Novoa, J. J.; Planas, M.; Rovira, M. C. *Chem. Phys. Lett.* **1996**, *251*, 33. Novoa, J. J.; Planas, M.; Whangbo, M.-H. *Chem. Phys. Lett.* **1994**, *186*, 175. Hobza, P.; Zahradnik, R. *Chem. Rev.* **1988**, *88*, 871. Scheiner, S. *Rev. Comput. Chem.* **1991**, *2*, 165.
(42) Kim, K.; Jordan, K. D. *J. Phys. Chem.* **1994**, *98*, 10089.
(43) Novoa, J. J.; Sosa, C. *J. Phys. Chem.* **1995**, *99*, 15837.
(44) Boys S. F.; Bernardi F. *Mol. Phys.* **1970** *19*, 553.